



# A model for extreme plasticity

S.J. Thomson\*, P.D. Howell

Mathematical Institute, University of Oxford Andrew Wiles Building, Woodstock Road, Oxford OX2 6GG, UK

## ARTICLE INFO

### Article history:

Received 29 February 2016

Received in revised form

4 April 2016

Accepted 7 April 2016

Available online 13 May 2016

### Keywords:

Elastoplasticity

Equation of state

Asymptotic analysis

## ABSTRACT

We present a mathematical model for elastoplasticity in the regime where the applied stress greatly exceeds the yield stress. This scenario is typically found in violent impact testing, where millimetre thick metal samples are subjected to pressures on the order of  $10\text{--}10^2$  GPa, while the yield stress can be as low as  $10^{-2}$  GPa. In such regimes the metal can be treated as a barotropic compressible fluid in which the strength, measured by the ratio of the yield stress to the applied stress, is negligible to lowest order. Our approach is to exploit the smallness of this ratio by treating the effects of strength as a small perturbation to a leading order barotropic model. We find that for uniaxial deformations, these additional effects give rise to features in the response of the material which differ significantly from the predictions of barotropic flow.

© 2016 The Authors. Published by Elsevier Ltd. This is an open access article under the CC BY license (<http://creativecommons.org/licenses/by/4.0/>).

## 1. Introduction

Most simulations of the mechanical response of a metal undergoing violent elastic–plastic deformation rely on knowledge of the equation of state (EoS) for the material under study. Traditionally, shock waves generated using a gas-gun have been used to determine this information theoretically and experimentally (Davison and Graham, 1979; Molinari and Ravichandran, 2004; Meyers, 1994; Davison, 2008; Clifton, 1985; Germain and Lee, 1973). More recently, the so-called isentropic compression experiments (ICEs) have become a standard method by which we extract EoS information in the absence of shock waves (Davis, 2006; Rothman et al., 2014, 2005). There are several advantages in using ICEs over shock wave experiments, one of which is that the entire isentrope can be obtained in a single experiment. In comparison, one shock wave experiment gives only one point on the Hugoniot, corresponding to a single value of the entropy. Multiple experiments are then required to generate the entire EoS. Another advantage is that the temperature in shock wave experiments can become sufficiently high to melt the material, while in ICEs the material remains in the solid phase. This allows EoS data for the solid phase to be obtained at much higher pressures.

A schematic of a typical experiment is shown in Fig. 1. Using a magnetic pressure drive, a ramped compression wave is made to propagate through the target sample. The target is designed to be thin compared to its lateral extent, so that waves generated at the outer edge of the sample do not have time to reach the centre during the time-scale of the experiment. Thus the material at the centre of the sample undergoes purely uniaxial deformation, with displacement varying only in the direction of impact. After a short time, the velocity at the rear face of the target material is recorded using velocity interferometry. The results from a typical experiment are shown in Fig. 2. When an attempt is made to reconstruct this velocity profile numerically by tuning certain parameters in the constitutive assumptions of the model, the problem becomes an

\* Corresponding author.

E-mail address: [thomson@maths.ox.ac.uk](mailto:thomson@maths.ox.ac.uk) (S.J. Thomson).

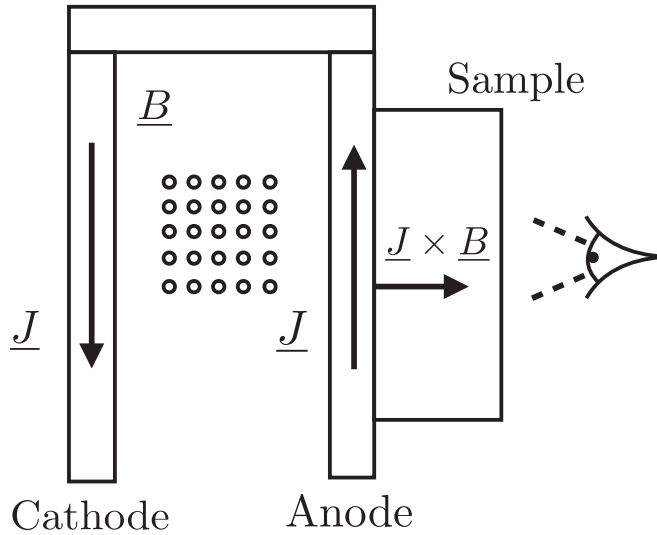


**Fig. 1.** Schematic of a ramped isentropic compression experiment. A current passes between the cathode and anode, perpendicular to a magnetic field directed into the page. The resulting Lorentz force provides a pressure drive against the front face of the target sample.

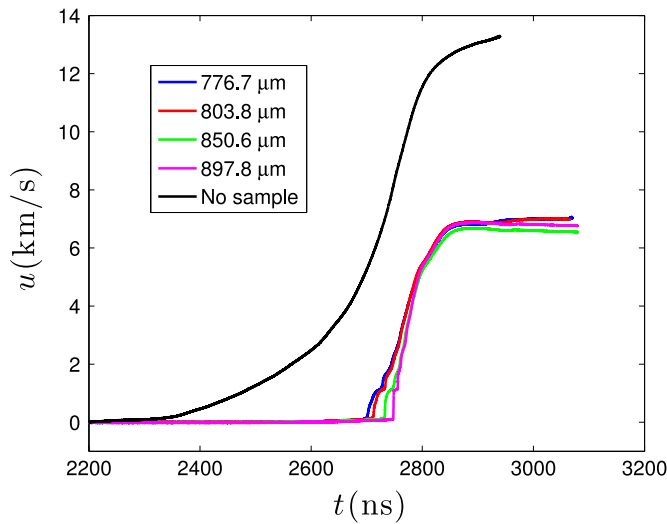


**Fig. 2.** Boundary velocimetry data obtained from 3 MBar compression of lead (Rothman et al., 2014). The coloured curves show the free-surface velocity  $u$  measured for different thicknesses of the sample. A reference curve with no lead sample is plotted in black. (For interpretation of the references to colour in this figure caption, the reader is referred to the web version of this paper.)

inverse problem for the equation of state.

Previous attempts to infer EoS information from such experiments have typically neglected the effects of mechanical strength, instead treating the material as a barotropic compressible fluid (Hinch, 2010; Ockendon et al., 2010). This approximation is based on the fact that, under extreme conditions, the ability of a solid object to resist shear is limited by the yield stress, which is typically much smaller than the applied stress. However, violent impact experiments reported by numerous authors have confirmed the existence of both elastic and plastic waves (Meyers, 1994; Clifton, 1985; Pack et al., 1948; Von Karman and Duwez, 1950; Whitley et al., 2011). The former propagate through the material as the stress increases toward the yield stress, and the latter as the material is compressed further beyond the yield surface. Therefore, a proper account of violent elastic–plastic deformation requires one to account for both the compressibility of the material and the small but measurable effects of elasticity.

There exist numerous macroscopic models in the literature pertaining to metal plasticity, which reflects the reality that no one theory of plasticity is universally accepted, in contrast to the theories of elasticity or fluid dynamics (Steinberg et al., 1980; Steinberg and Lund, 1989; Green and Naghdi, 1965; Willis, 1969; Howell et al., 2016, 2014; Plohr and Sharp, 1992). The key physical phenomenon underpinning plastic deformation is the nucleation and motion of dislocations (Orowan et al., 1954; Hirth and Lothe, 1982; Clifton and Markenscoff, 1981; Johnson and Barker, 1969). However, even on the length-scale of

a few millimetres there are a vast number of dislocations, occupying many possible configurations. Therefore, at realistic macroscopic length-scales, it is not feasible to track the motion of individual dislocations, and instead one must construct a continuum model that describes bulk elastoplastic deformation in an averaged way. Many such models aim to encapsulate a broad range of phenomena by fitting parameters in the constitutive assumptions of the model. However, such complexity bears a cost in that the resulting models are usually too complicated to be susceptible to a systematic mathematical analysis. Nevertheless, they often form the basis of computational hydrocodes used to determine properties such as the EoS of the material under study. It is therefore our aim to enhance the utility of such codes by constructing a model which is realistic, based on sound principles from mechanics and thermodynamics, but also simple enough to allow for a mathematical analysis of some configurations in impact mechanics, in particular uniaxial isentropic compression experiments.

In this paper, we present a new mathematical model of elastoplasticity in the regime where the applied stress greatly exceeds the yield stress. In the limit of zero yield stress, the model reduces to the equations of barotropic flow, while the effects of strength are treated as a small perturbation to this leading order model. Our systematic asymptotic analysis reveals that, in the absence of shocks, entropy changes are universally negligible despite the wide variations in stress, confirming suggestions made in [Wallace \(1980a,b,c\)](#).

This paper is organised as follows. In Section 2 we derive our model for extreme plasticity. Then in Section 3 we present numerical solutions of the governing equations to investigate the predictions of our model on the elastic and plastic waves that propagate through a metal sample during violent impact. We show that the inclusion of elastic effects gives rise to significant distinctive features in the material response which cannot be resolved by barotropic flow alone.

## 2. Mathematical model

### 2.1. Governing equations

Motivated by experimental evidence, we restrict our attention to one-dimensional, uniaxial strain where a material particle initially at Lagrangian position  $(X, Y, Z)$  is displaced to Eulerian position  $(x(X, t), Y, Z)$  after time  $t$ . We begin by defining the stretch  $\nu$  and the axial velocity  $u$  by

$$\nu = \frac{\partial x}{\partial X} = \frac{\rho_0}{\rho}, \quad u = \frac{\partial x}{\partial t},$$

where  $\rho$  is the density and the initial density  $\rho_0$  is assumed to be constant. These two quantities are related by the kinematic equation

$$\frac{\partial \nu}{\partial t} - \frac{\partial u}{\partial X} = 0. \quad (1)$$

We make the common assumption that the total deformation gradient may be decomposed multiplicatively into an elastic and plastic part. In one-dimensional deformation, this leads to

$$\mathbf{F} = \text{diag}(\nu, 1, 1) = \mathbf{F}^e \mathbf{F}^p,$$

where the elastic and plastic deformations are each assumed to be uniaxial, so that

$$\mathbf{F}^e = \text{diag}(F_1^e, F_2^e, F_2^e), \quad \mathbf{F}^p = \text{diag}(F_1^p, F_2^p, F_2^p).$$

We thus obtain the relations

$$F_1^e F_1^p = \nu, \quad F_2^e F_2^p = 1. \quad (2)$$

Since we are considering uniaxial deformation, the Cauchy stress tensor is of the form

$$\boldsymbol{\sigma} = \text{diag}(\sigma_1(X, t), \sigma_2(X, t), \sigma_2(X, t)).$$

The conservation of momentum equation then reads

$$\rho_0 \frac{\partial u}{\partial t} - \frac{\partial \sigma_1}{\partial X} = 0. \quad (3)$$

Provided there are no heat sources and thermal conduction is negligible, the equation for conservation of energy reads

$$\frac{\partial}{\partial t} \left( \frac{1}{2} \rho_0 u^2 + \mathcal{W} \right) - \frac{\partial}{\partial X} (u \sigma_1) = 0 \quad (4)$$

where  $\mathcal{W}$  is the internal energy per unit reference volume. Expanding out (4) and using (1) and (3), we can alternatively write

$$\frac{\partial \mathcal{W}}{\partial t} = \sigma_1 \frac{\partial \nu}{\partial t}. \quad (5)$$

We now assume that  $\mathcal{W}$  is a function of the elastic deformation gradients  $F_1^e$ ,  $F_2^e$  and the entropy  $S$ . The stress components and the temperature  $T$  are then derivable from  $\mathcal{W}$  using

$$T = \frac{1}{\rho_0} \frac{\partial \mathcal{W}}{\partial S}, \quad \sigma_1 = \frac{F_1^e}{\nu} \frac{\partial \mathcal{W}}{\partial F_1^e}, \quad \sigma_2 = \frac{F_2^e}{2\nu} \frac{\partial \mathcal{W}}{\partial F_2^e}, \quad (6)$$

where the factor of 2 in the expression for  $\sigma_2$  arises from the assumption of uniaxiality. Later we will specialise the form of  $\mathcal{W}$  to one suitable to problems of large plastic deformation. Using the relations (2) and (6) we can write the energy equation (5) in the form

$$\rho_0 T \frac{\partial S}{\partial t} = \frac{2\nu(\sigma_1 - \sigma_2)}{F_2^e} \frac{\partial F_2^e}{\partial t}. \quad (7)$$

To close the model, we need to specify a flow rule for the irreversible plastic flow which occurs when the stress in the material reaches and possibly exceeds the yield stress. Following Howell et al. (2009), we define

$$\frac{1}{F_1^p} \frac{\partial F_1^p}{\partial t} = - \frac{2}{F_2^p} \frac{\partial F_2^p}{\partial t} = \Lambda \operatorname{sign}(\sigma_1 - \sigma_2). \quad (8)$$

A first integral of these equations ensures that the plastic flow is incompressible, that is

$$F_1^p F_2^{p2} = 1, \quad (9)$$

and that the dissipation is non-negative provided the flow rate  $\Lambda$  is non-negative. While the deviatoric stress is below the yield stress  $\sigma_Y$ , the material is assumed to be elastic, with  $\Lambda = 0$ . In rate-independent perfect plasticity, the deviatoric stress is precisely equal to the yield stress during plastic flow. However, in violent impact experiments this strict yield criterion may be violated, and we expect the plastic flow rate  $\Lambda$  to be an increasing function of the amount by which the deviatoric stress exceeds the yield stress. We therefore pose the flow rule

$$\Lambda = r \left[ \frac{|\sigma_1 - \sigma_2|}{\sigma_Y} - 1 \right]^+ \quad (10)$$

where

$$[x]^+ = \begin{cases} 0 & \text{if } x \leq 0, \\ x & \text{if } x > 0, \end{cases}$$

and  $r$  is a rate constant with units of inverse time. Models of this type are well-substantiated and may be found in the literature as far back as Perzyna (1966).

Combining Eqs. (8) and (11), we obtain the following rule for the plastic strain rate:

$$\frac{1}{F_1^p} \frac{\partial F_1^p}{\partial t} = rG \left( \frac{\sigma_1 - \sigma_2}{\sigma_Y} \right), \quad (11)$$

where

$$G(z) = z + \frac{1}{2}|z - 1| - \frac{1}{2}|z + 1|$$

as shown in Fig. 3. Eq. (11) reduces to rate-independent perfect plasticity in the limit  $r \rightarrow \infty$ .

To summarise, once we have specified a form for  $\mathcal{W}$ , Eqs. (1), (2), (3), (6), (7), (9) and (11) provide a system of nine scalar equations for the nine unknowns  $\nu$ ,  $u$ ,  $S$ ,  $F_1^e$ ,  $F_2^e$ ,  $F_1^p$ ,  $F_2^p$ ,  $\sigma_1$  and  $\sigma_2$ .

## 2.2. Equation of state

Our model is closed by specifying a constitutive law for the energy density function  $\mathcal{W}$ . For the material to undergo large plastic deformations with  $O(1)$  variations in density, we see from (1) and (3) that the axial stress must be  $O(\rho_0 c_0^2)$  where  $c_0$  is a typical sound speed. However, the flow rule (11) implies that the deviatoric stress  $\sigma_1 - \sigma_2$  is of order  $\sigma_Y$ , which is typically much smaller. This in turn implies that, although the net volumetric deformation  $\nu$  may undergo  $O(1)$  variations, the deviatoric elastic strain is expected to be much smaller. Using (2), it is therefore useful to define

$$F_1^e = \nu^{1/3} \sqrt{1 + 2\mathcal{E}}, \quad F_2^e = \frac{\nu^{1/3}}{(1 + 2\mathcal{E})^{1/4}},$$

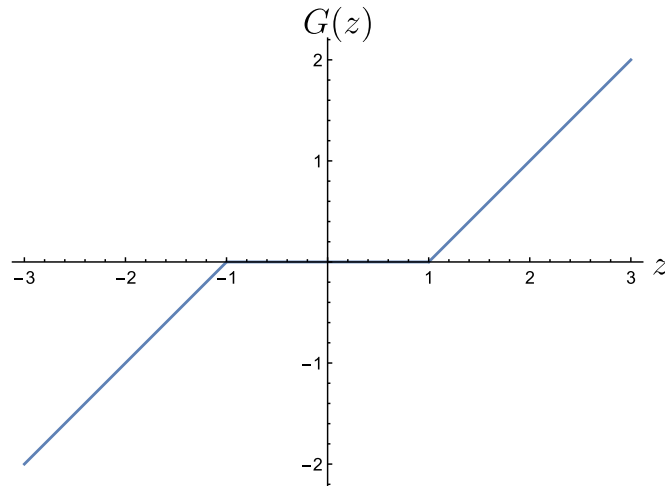


Fig. 3. Plot of the yield function  $G$ .

where  $\mathcal{E}$  is a measure of the deviatoric elastic strain, and we anticipate that  $|\mathcal{E}| \ll 1$  while  $\nu = O(1)$ .

If we now think of  $\mathcal{W}$  as a function of  $\nu$ ,  $\mathcal{E}$ ,  $S$ , we can use (6) to express the stress components as

$$\sigma_1 = \frac{\partial \mathcal{W}}{\partial \nu} + \frac{2(1+2\mathcal{E})}{3\nu} \frac{\partial \mathcal{W}}{\partial \mathcal{E}}, \quad \sigma_1 - \sigma_2 = \frac{1+2\mathcal{E}}{\nu} \frac{\partial \mathcal{W}}{\partial \mathcal{E}}. \quad (12)$$

The energy equation (5) then becomes

$$\frac{\partial \mathcal{W}}{\partial S} \frac{\partial S}{\partial t} = \frac{\partial \mathcal{W}}{\partial \mathcal{E}} \left( \frac{2(1+2\mathcal{E})}{3\nu} \frac{\partial \nu}{\partial t} - \frac{\partial \mathcal{E}}{\partial t} \right), \quad (13)$$

and the rate-dependent flow rule (8) becomes

$$\frac{2}{3\nu} \frac{\partial \nu}{\partial t} - \frac{1}{1+2\mathcal{E}} \frac{\partial \mathcal{E}}{\partial t} = rG \left( \frac{1+2\mathcal{E}}{\sigma_Y \nu} \frac{\partial \mathcal{W}}{\partial \mathcal{E}} \right). \quad (14)$$

As discussed above, we expect the deviatoric elastic strain to be small, specifically of order

$$\delta = \frac{\sigma_{Y0}}{\rho_0 c_0^2} \ll 1$$

where  $\sigma_{Y0}$  denotes a representative value of  $\sigma_Y$  to allow for situations in which  $\sigma_Y$  varies with  $\nu$ , for example. This motivates us to define

$$\epsilon = \frac{\mathcal{E}}{\delta} = O(1).$$

We can therefore expand  $\mathcal{W}(\nu, \mathcal{E}, S)$  in a Taylor series of the form

$$\frac{\mathcal{W}}{\rho_0 c_0^2} \sim \mathcal{W}_0(\nu, S) + \delta^2 \mathcal{W}_2(\nu, S) \epsilon^2 + O(\delta^3), \quad (15)$$

where we assume that  $\epsilon = 0$  is a local minimum of the elastic energy. The term  $\mathcal{W}_0$  is the leading order, thermodynamic part of the equation of state, while  $\mathcal{W}_2$  is analogous to the shear modulus of the material. A similar expansion was suggested in Willis (1969, Eq. 4.18).

From Eq. (13) we now infer that, in the absence of shocks, the entropy production through dissipation is small, so that

$$S = S_0(1 + \delta s) \quad (16)$$

where  $s = O(1)$  and the initial entropy  $S_0$  is assumed to be constant. We can therefore restrict Eq. (15) further to

$$\frac{\mathcal{W}}{\rho_0 c_0^2} \sim h(\nu) + \delta s \theta(\nu) + \delta^2 \left( s^2 S_0^2 \frac{\partial^2 \mathcal{W}_0}{\partial S^2}(S_0, \nu) + \frac{1}{2} k(\nu) \epsilon^2 \right) + O(\delta^3), \quad (17)$$

where

$$h(\nu) = \mathcal{W}_0(S_0, \nu), \quad \theta(\nu) = S_0 \frac{\partial \mathcal{W}_0}{\partial S}(S_0, \nu), \quad k(\nu) = 2\mathcal{W}_2(S_0, \nu).$$

Finally, we find the following approximations for the stress components:

$$\frac{\sigma_1}{\rho_0 c_0^2} \sim h'(\nu) + \delta \left( s\theta'(\nu) + \frac{2k(\nu)}{3\nu} \epsilon \right) + O(\delta^2), \quad \frac{\sigma_1 - \sigma_2}{\sigma_{Y0}} \sim \frac{k(\nu)}{\nu} \epsilon + O(\delta). \quad (18)$$

We note that Eq. (18) for the longitudinal stress  $\sigma_1$  is related to the Mie–Grüneisen equation of state, with  $h'(\nu)$  identified with the isotropic pressure, while the  $O(\delta)$  terms are the small contributions from temperature and shear strength respectively (Davison, 2008; Gathers, 1994).

### 2.3. Non-dimensionalisation

We non-dimensionalise the governing equations as follows:

$$X = LX', \quad t = \frac{L}{c_0} t', \quad u = c_0 u',$$

where  $L$  is a typical sample thickness. Henceforth we drop the prime notation to reduce clutter. In dimensionless form, the governing equations (1), (3), (13) and (14) in the limit  $\delta \rightarrow 0$  reduce to

$$\frac{\partial \nu}{\partial t} - \frac{\partial u}{\partial X} = 0, \quad (19)$$

$$\frac{\partial u}{\partial t} - h''(\nu) \frac{\partial \nu}{\partial X} = 0, \quad (20)$$

$$\theta(\nu) \frac{\partial s}{\partial t} = \frac{2k(\nu)}{3\nu} \frac{\partial \nu}{\partial t}, \quad (21)$$

$$\frac{2a}{3\nu} \frac{\partial \nu}{\partial t} = G\left(\frac{\epsilon}{\epsilon_c(\nu)}\right), \quad (22)$$

where

$$\epsilon_c(\nu) = \frac{\nu \sigma_Y(\nu)}{\sigma_{Y0} k(\nu)}$$

represents the normalised yield strain, and

$$a = \frac{c_0}{rL}$$

is a dimensionless relaxation time for the stress to relax to the yield surface.

### 2.4. Small amplitude oscillations

Eqs. (19) and (20) satisfied by the specific volume  $\nu$  and the velocity  $u$  are equivalent to the equations of one-dimensional barotropic flow. The entropy change  $\delta s$  and the normalised deviatoric strain  $\epsilon$  are then determined in principle by the decoupled energy equation (21) and the flow rule (22). However, the form of the function  $G$  means that Eq. (22) is degenerate when the left-hand side is zero, which suggests the existence of a distinguished asymptotic limit when  $\partial \nu / \partial t$  is small.

To examine the behaviour of the governing equations when the displacement is small, we perform the re-scalings

$$\nu = 1 + \delta \eta, \quad u = \delta U, \quad s = \delta \zeta$$

before taking limit  $\delta \rightarrow 0$ . The leading order governing equations in this regime are

$$\frac{\partial \eta}{\partial t} - \frac{\partial U}{\partial X} = 0, \quad (23)$$

$$\frac{\partial U}{\partial t} - \frac{\partial \eta}{\partial X} - \frac{2k_0}{3} \frac{\partial \epsilon}{\partial X} = 0, \quad (24)$$

$$\theta(1) \frac{\partial \zeta}{\partial t} = k_0 \epsilon \left( \frac{2}{3} \frac{\partial \eta}{\partial t} - \frac{\partial \epsilon}{\partial t} \right), \quad (25)$$

$$a\delta\left(\frac{2}{3}\frac{\partial\eta}{\partial t}-\frac{\partial\epsilon}{\partial t}\right)=G(\epsilon), \quad (26)$$

where  $k_0 = k(1)$ , and we assume  $h''(1) = \epsilon_c(1) = 1$  by the choice of scalings  $c_0$  and  $\sigma_{Y0}$ . If  $a\delta = O(1)$ , then Eqs. (23), (24) and (26) provide a coupled semilinear hyperbolic system for  $\eta$ ,  $\nu$  and  $\epsilon$ , while the entropy change  $\delta^2\zeta$  is again negligible to lowest order and may be determined a posteriori from Eq. (25).

### 2.5. Uniformly valid model

All of the preceding analysis suggests that in the regime  $\delta \ll 1$ , entropy variations from its initially constant value are universally negligible in the absence of shocks, and a uniformly valid model which captures all of the above behaviour is

$$\frac{\partial\nu}{\partial t}-\frac{\partial u}{\partial X}=0, \quad (27)$$

$$\frac{\partial u}{\partial t}-\frac{\partial}{\partial X}\left(h'(\nu)+\frac{2\delta k(\nu)}{3\nu}\epsilon\right)=0, \quad (28)$$

$$a\left(\frac{2}{3\nu}\frac{\partial\nu}{\partial t}-\delta\frac{\partial\epsilon}{\partial t}\right)=G\left(\frac{\epsilon}{\epsilon_c(\nu)}\right). \quad (29)$$

Eqs. (27)–(29) reduce to the equations of barotropic flow in the limit  $\delta \rightarrow 0$ . In regions where the strain is  $O(1)$ , the terms of  $O(\delta)$  just give rise to small elastic corrections to the dominant barotropic flow. However in regions where the strain is  $O(\delta)$ , the deviatoric and isotropic contributions to the strain are comparable, and hence we expect elastic effects to be particularly significant near the tails of propagating plastic waves.

## 3. Numerical solutions

We now study the predictions of our model for the elastic and plastic waves that propagate through a metal sample when subjected to a compressive force at  $X=0$ . The governing partial differential equations (27)–(29) are of hyperbolic type, so we use the method of Kurganov and Tadmor (2000) to compute numerical solutions.

The simplest initial and boundary conditions that we can impose to simulate violent compression are

$$\nu = 1, \quad u = 0, \quad \epsilon = 0 \text{ at } t = 0, \quad X > 0, \quad (30)$$

$$u = U_0(1 - e^{-t}) \text{ at } X = 0, \quad t > 0. \quad (31)$$

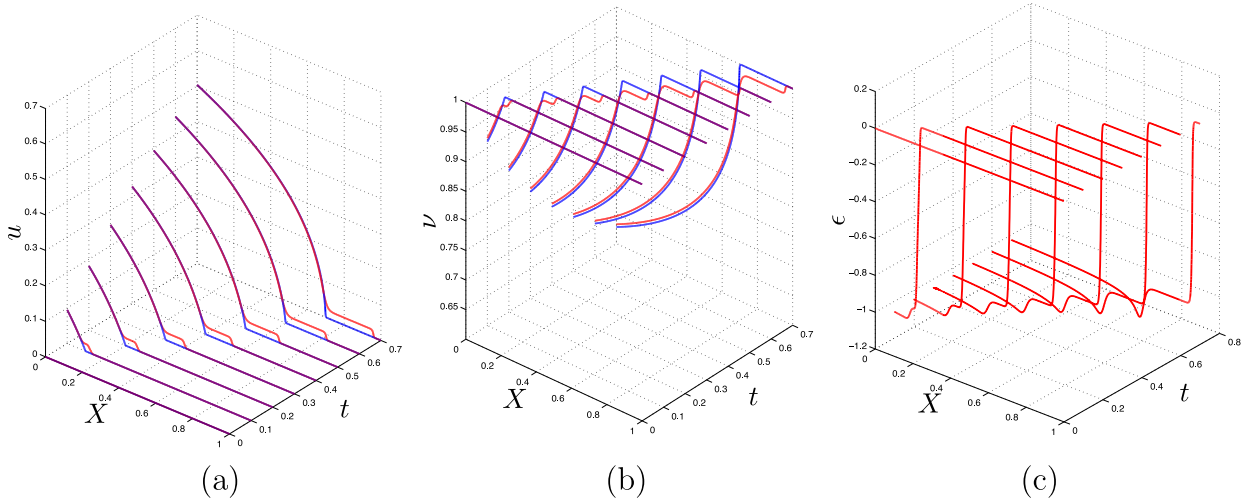
These correspond to a semi-infinite initially undisturbed sample in  $X > 0$  subject to an imposed velocity at the face  $X=0$  which ramps up to a constant value  $U_0$ . To proceed, we also need to make specific choices for the constitutive functions  $h$ ,  $k$  and  $\epsilon_c$ . A wide variety of empirical constitutive relations may be found in the literature (see e.g. Davison, 2008). For simplicity, and to compare with a leading order barotropic flow model that resembles homentropic gas dynamics, we make the following constitutive assumptions:

$$h(\nu) = \frac{1}{\gamma(\gamma-1)\nu^{\gamma-1}}, \quad k(\nu) = K, \quad \epsilon_c(\nu) = 1,$$

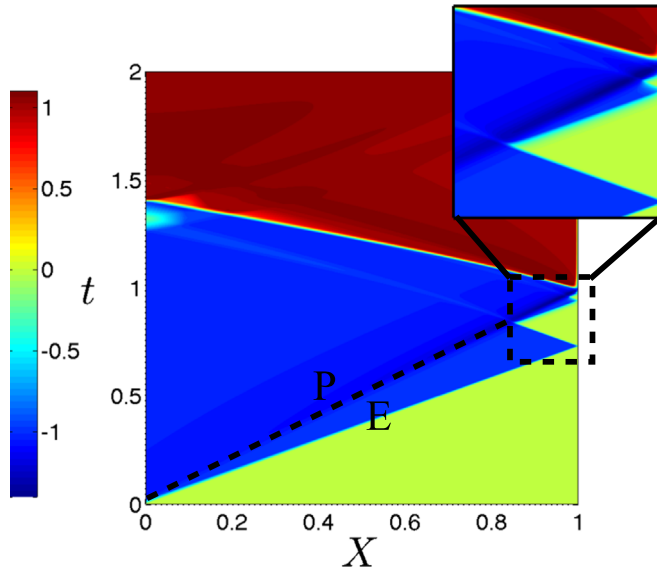
where  $\gamma > 1$  and  $K > 0$  are constants.

Fig. 4 shows plots of numerical solutions for (a) the velocity  $u(X, t)$ , (b) the specific volume  $\nu(X, t)$ , and (c) the deviatoric strain  $\epsilon(X, t)$ . The red curves show solutions to the full elastoplastic model (27)–(31), while the blue curves in (a) and (b) show the corresponding solutions of the barotropic flow model, where  $\delta$  is set to zero. These blue curves show the expected propagation of a large-amplitude plastic wave into the undisturbed material as the velocity at  $X=0$  is ramped up. Initially, the elastoplastic solution remains close to the barotropic flow prediction, apart from a small elastic precursor wave which propagates ahead of the much larger plastic wave. This confirms our expectation that elastic effects should be noticeable in regions where the strain is small, while plastic effects dominate wherever the strain is  $O(1)$ . Fig. 4(c) shows that the deviatoric strain varies rapidly from zero to  $-1$  across the elastic wavefront. Between the elastic and plastic wavefronts, there is a “plateau” region where  $\epsilon \approx -1$  and the material remains close to the yield surface, before fully yielding when the plastic wave arrives.

In ICEs, the quantity which can be measured is the velocity of the stress-free end of the target material upon the arrival of the incident elastic and plastic waves. To model such experiments, we solve the model (27)–(31) on a finite domain  $X \in [0, 1]$  subject to the additional boundary condition



**Fig. 4.** The red curves show numerical solutions of the problem (27)–(31) for (a) velocity  $u$ , (b) specific volume  $\nu$ , (c) deviatoric strain  $\epsilon$ , plotted versus Lagrangian position  $X$  at times  $t = 0, 0.1, \dots, 0.7$ . The parameter values are  $U_0 = 1$ ,  $\gamma = 5/3$ ,  $K = 2$ ,  $a = 0.1$ ,  $\delta = 0.01$ . In (a) and (b), the blue curves show the corresponding results for the barotropic flow model (with  $\delta = 0$ ). (For interpretation of the references to colour in this figure caption, the reader is referred to the web version of this paper.)



**Fig. 5.** Numerical solution of the model (27)–(32) for the deviatoric strain  $\epsilon(X, t)$ , using the same parameter values as in Fig. 4. (Online version in colour.)

$$\sigma_1(1, t) = \left[ h'(\nu) + \frac{2\delta k(\nu)}{3\nu} \epsilon \right]_{X=1} = 0. \quad (32)$$

The dynamics of the elastic waves are best visualised through the deviatoric strain  $\epsilon$ . Fig. 5 shows a heat map of  $\epsilon(X, t)$  for  $X \in (0, 1)$  and  $t \in (0, 2)$ , computed using the elastoplastic model (27)–(32) with the same parameter values as in Fig. 4. The material is undisturbed where  $\epsilon = 0$ , elastic where  $|\epsilon| < 1$  and plastic where  $|\epsilon| \geq 1$ . Initially an elastic wave, labelled E, propagates ahead of a plastic wave of much larger amplitude, labelled P. When the elastic wave reaches the free surface at  $X = 1$ , it reflects back toward the incoming plastic wave. During the interaction of the two waves (see the inset), part of the elastic wave is transmitted through the plastic wave, while part is reflected back toward the free surface. The elastic wave thus reverberates back and forth until the eventual arrival of the large amplitude plastic wave at the free surface. We note that there is always an unyielded region close to the free surface  $X = 1$  and that, while they are not interacting, the elastic and plastic waves are separated by a plateau region in which  $|\epsilon| \approx 1$  and the material sits approximately on the yield surface.

The velocity at the free surface  $u(1, t)$  is plotted in red in Fig. 6, and compared with the corresponding results for

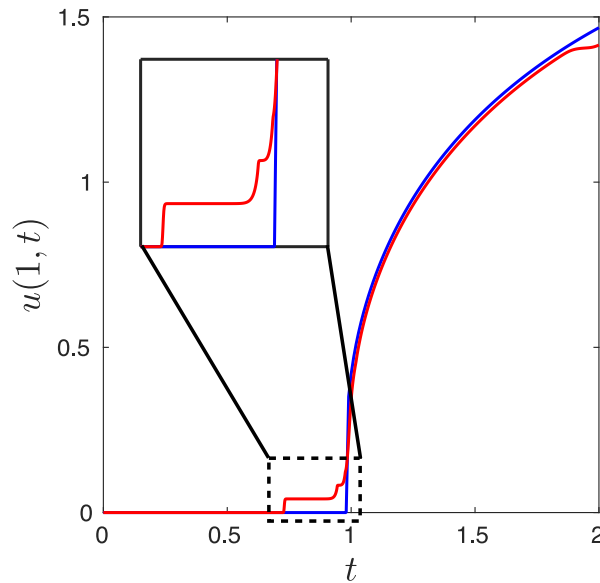


**Fig. 6.** Free-surface velocity  $u(1, t)$  computed using the elastoplastic model (27)–(32) (red); corresponding barotropic flow solution (blue). (For interpretation of the references to colour in this figure caption, the reader is referred to the web version of this paper.)

barotropic flow ( $\delta = 0$ , in blue). A small elastic precursor arrives ahead of the large plastic wave, and the reverberation leads to a staircase-like feature, with the velocity increasing through a series of small steps. Furthermore, it appears that the repeated interactions with the elastic waves degrade the plastic wave, resulting in a noticeable reduction in the final surface velocity at  $t=2$ . None of these significant features can be explained or resolved by a barotropic flow model alone.

#### 4. Conclusions

We have developed a one-dimensional model for elastoplasticity in the regime where the applied stress greatly exceeds the yield stress. This ratio is manifested in the non-dimensional parameter  $\delta$  which is assumed to be small throughout. Our model is valid in the absence of shocks, and this is important as ICEs are designed in such a way that shock formation occurs outwith the lifetime of the experiment. However, in principle, the methodology we apply here may be easily generalised to incorporate shocks by reinstating the energy equation (4) to account for jumps in the entropy  $S$ .

By studying the behaviour of our model in a scenario relevant to isentropic compression experiments we have found that it reveals several key features. These are that large scale plastic compression waves, which are approximately described by a barotropic flow model, are accompanied by small amplitude but fast moving elastic waves. Although the elastic waves are small, repeated interactions between the elastic and plastic waves may result in significant cumulative effects which cannot be explained by a purely barotropic theory. For example, Fig. 6 indicates a non-zero velocity at the free-surface *before* the arrival of the plastic wave, which would be impossible in purely barotropic flow. It is the subject of current work to quantify the structure of these interactions mathematically, so that they may be incorporated into a more accurate method for deriving EoS approximations from experimental boundary velocimetry data.

#### Acknowledgements

The authors would like to thank Dr. D.J. Allwright, Prof. J.R. Ockendon, Dr. Hilary Ockendon, Dr. C. Robinson, and Dr. J. Turner, for many helpful discussions and suggestions. S.J.T. would also like to thank Rothman et al. (2014) for providing the experimental data used in Fig. 2. This work was funded under the CASE studentship EP/I501592/1 with joint funding from EPSRC and AWE plc. In compliance with the EPSRC's open access initiative, the data in this paper is available from <http://dx.doi.org/10.5287/bodleian:5zBZ7Vq2E>.

#### References

- Clifton, R., Markenscoff, X., 1981. Elastic precursor decay and radiation from nonuniformly moving dislocations. *J. Mech. Phys. Solids* 29 (3), 227–251.
- Clifton, R.J., 1985. Stress wave experiments in plasticity. *Int. J. Plast.* 1 (4), 289–302.
- Davis, J.-P., 2006. Experimental measurement of the principal isentrope for aluminum 6061-T6 to 240 GPa. *J. Appl. Phys.* 99 (10), 103512.

- Davison, L., Graham, R.A., 1979. Shock compression of solids. *Phys. Rep.* 55 (4), 255–379.
- Davison, L., 2008. *Fundamentals of Shock Wave Propagation in Solids*. Springer Science & Business Media, Berlin, Germany.
- Gathers, G.R., 1994. *Selected Topics in Shock Wave Physics and Equation of State Modelling*. World Scientific, New York, Singapore.
- Germain, P., Lee, E., 1973. On shock waves in elastic–plastic solids. *J. Mech. Phys. Solids* 21 (6), 359–382.
- Green, A.E., Naghdi, P.M., 1965. A general theory of an elastic–plastic continuum. *Arch. Ration. Mech. Anal.* 18 (4), 251–281.
- Hinch, E.J., 2010. Determining the equation of state of highly plasticised metals from boundary velocimetry. *J. Eng. Math.* 68 (3), 279–289.
- Hirth, J.P., Lothe, J., 1982. *Theory of Dislocations*.
- Howell, P.D., Kozyreff, G., Ockendon, J.R., 2009. *Applied Solid Mechanics*. Cambridge University Press, Cambridge, UK.
- Howell, P.D., Ockendon, H., Ockendon, J.R., 2014. An asymptotic model for elastoplasticity. *J. Eng. Math.* 84 (1), 57–71.
- Howell, P.D., Ockendon, H., Ockendon, J.R., 2012. Mathematical modelling of elastoplasticity at high stress. *Proc. R. Soc. A.* 468, 3842–3868.
- Johnson, J., Barker, L., 1969. Dislocation dynamics and steady plastic wave profiles in 6061-t6 aluminum. *J. Appl. Phys.* 40 (11), 4321–4334.
- Kurganov, A., Tadmor, E., 2000. New high-resolution central schemes for nonlinear conservation laws and convection–diffusion equations. *J. Comput. Phys.* 160 (1), 241–282, Berlin, Germany.
- Meyers, M., 1994. *Dynamic Behaviour of Materials*. John Wiley & Sons, New York.
- Molinari, A., Ravichandran, G., 2004. Fundamental structure of steady plastic shock waves in metals. *J. Appl. Phys.* 95 (4), 1718–1732.
- Ockendon, H., Ockendon, J.R., Platt, J., 2010. Determining the equation of state of highly plasticised metals from boundary velocimetry: Part I. *J. Eng. Math.* 68 (3–4), 269–277.
- Orowan, E., et al., 1954. *Dislocations in Metals*. AIME, New York, p. 131.
- Pack, D., Evans, W., James, H., 1948. The propagation of shock waves in steel and lead, *Proc. Phys. Soc.* 60 (1) 1.
- Perzyna, P., 1966. Fundamental problems in viscoplasticity. *Adv. Appl. Mech.* 9, 243.
- Plohr, B.J., Sharp, D.H., 1992. A conservative formulation for plasticity. *Adv. Appl. Math.* 13 (4), 462–493.
- Rothman, S., Davis, J., Maw, J., Robinson, C., Parker, K., Palmer, J., 2005. Measurement of the principal isentropes of lead and lead-antimony alloy to ~400 kbar by quasi-isentropic compression. *J. Phys. D: Appl. Phys.* 38 (5), 733.
- Rothman, S., Davis, J., Gooding, S., Knudson, M., Ao, T., 2014. Measurement of the principal quasi-isentrope of lead to 3 megabar using the z-machine. *J. Phys.: Conf. Ser.* 500, 032016.
- Steinberg, D., Lund, C., 1989. A constitutive model for strain rates from  $10^{-4}$  to  $10^6 \text{ s}^{-1}$ . *J. Appl. Phys.* 65 (4), 1528–1533.
- Steinberg, D., Cochran, S., Guinan, M., 1980. A constitutive model for metals applicable at high-strain rate. *J. Appl. Phys.* 51 (3), 1498–1504.
- Von Karman, T., Duwez, P., 1950. The propagation of plastic deformation in solids. *J. Appl. Phys.* 21 (10), 987–994.
- Wallace, D.C., 1980a. Equation of state from weak shocks in solids. *Phys. Rev. B* 22 (4), 1495.
- Wallace, D.C., 1980b. Flow process of weak shocks in solids. *Phys. Rev. B* 22 (4), 1487.
- Wallace, D.C., 1980c. Irreversible thermodynamics of flow in solids. *Phys. Rev. B* 22 (4), 1477.
- Whitley, V., McGrane, S., Eakins, D., Bolme, C., Moore, D., Bingert, J., 2011. The elastic–plastic response of aluminum films to ultrafast laser-generated shocks. *J. Appl. Phys.* 109 (1), 013505.
- Willis, J., 1969. Some constitutive equations applicable to problems of large dynamic plastic deformation. *J. Mech. Phys. Solids* 17 (5), 359–369.